11 F-18 Fluoride Bone Scintigraphy

Bhushan Desai and Peter S. Conti

Prostate Cancer

Case 11.1

An 81-year-old male with metastatic adenocarcinoma of prostate, status postradiation therapy, presenting with widespread osseous metastatic disease involving predominantly T4–T7 vertebral bodies along with posterior ribs from T4–T6, likely representing epidural disease with perineural spread (Fig. 11.1). There are also small lesions involving the right lamina T10, proximal right 9th and 10th ribs, L-4 vertebral bodies, and bilateral posterior ilium.

Case 11.2

A 75-year-old male diagnosed with metastatic adenocarcinoma of prostate, presenting with multiple foci of hypermetabolic and sclerotic osseous lesions involving L1, L3, right posterior L4, T12, and left T9 vertebral bodies (Fig. 11.2). Also noted is activity with faint sclerosis in the right anterior iliac bone and posterior left acetabulum.

Case 11.3

A 73-year-old male with history of prostatic adenocarcinoma, presenting with multiple hypermetabolic, predominantly sclerotic osseous lesions i nvolving the left temporal bone, right occipital bone, L1 vertebra, spinous process of L2, left iliac bone, and right iliac bone (Fig. 11.3).

P.S. Conti, A. Kaushik (eds.), *PET-CT*, DOI 10.1007/978-1-4419-5811-2_11

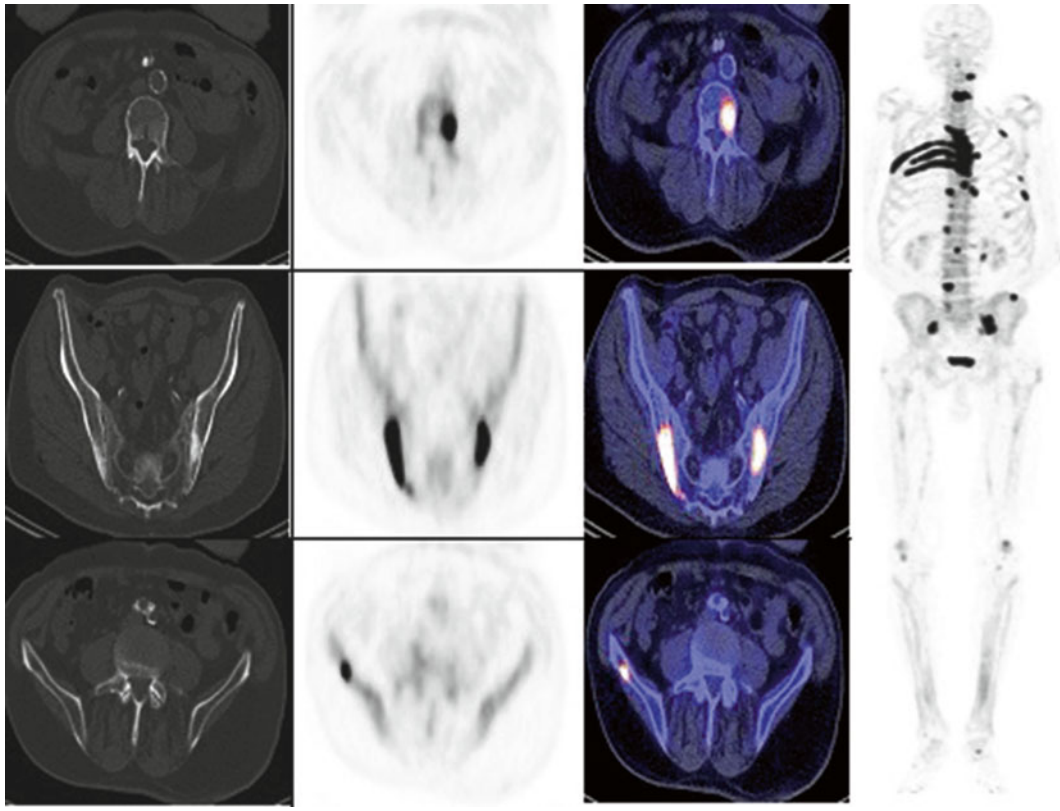

Fig. 11.1

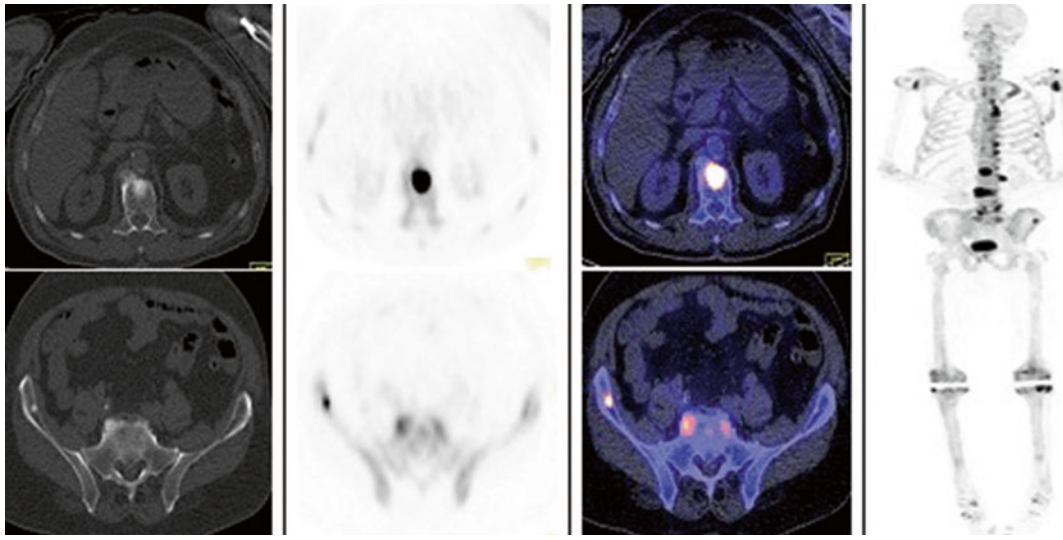

Fig. 11.2

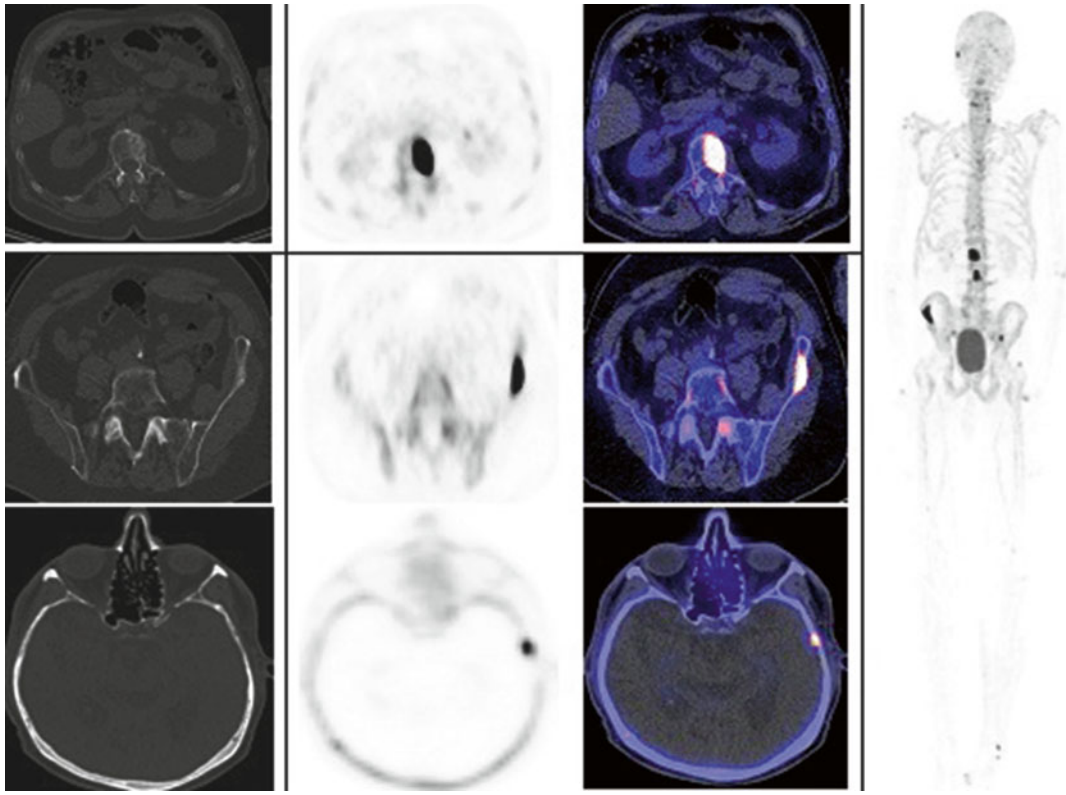

Fig. 11.3

Case 11.4 A 64-year-old male with biochemically recurrent prostate cancer, post radical prostatectomy, and EBRT, presenting with faintly sclerotic but intensely hypermetabolic right L2 metastatic lesion (Fig. 11.4). Tc99m MDP bone scintigraphy was negative. Other nonneoplastic findings include T11 osteophytic activity, Paget's-related increased right hemipelvis activity, and degenerative changes in the knees.

Breast Cancer

Case 11.5 A 54-year-old female with breast cancer presenting with hypermetabolic, predominantly sclerotic osseous lesions noted in T11, right C7 lamina, inferior L4 and sacral promontory, several ribs, left posterior pillar of acetabulum, and right posterior iliac disease (Fig. 11.5).

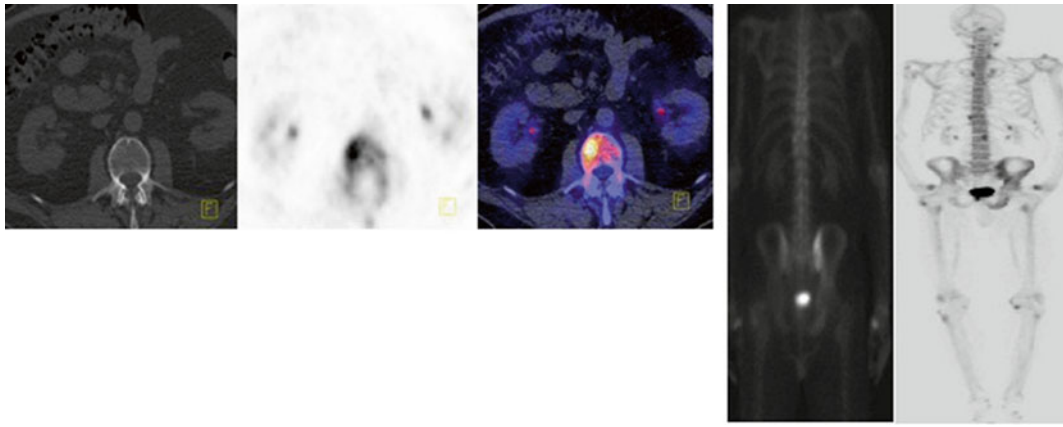

Fig. 11.4

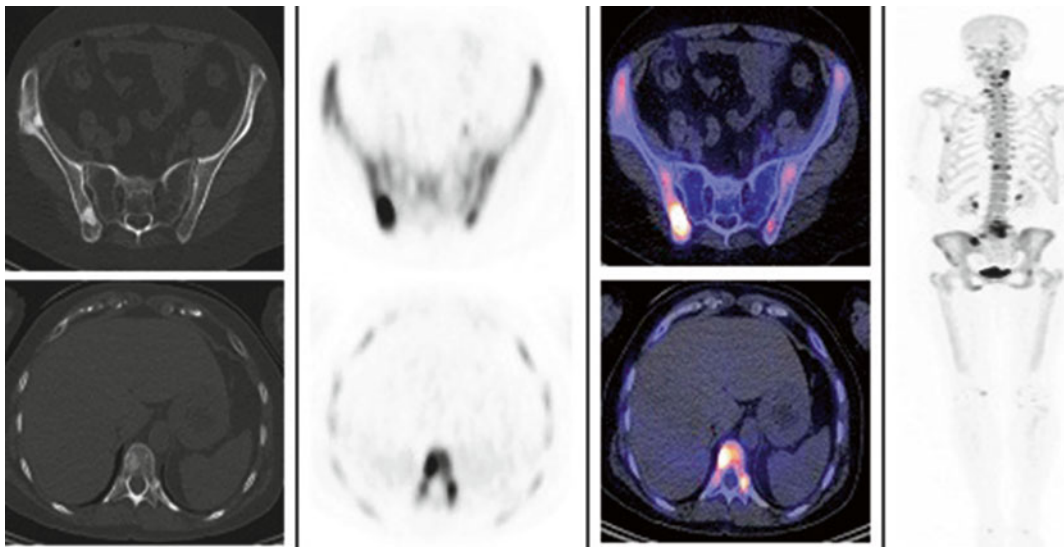

Fig. 11.5

Case 11.6

A 68-year-old female with history of metastatic right breast carcinoma, post right lumpectomy with axillary lymph node dissection, and right lung VATS procedure with talc pleurodesis, presenting with several hypermetabolic osseous lesions seen predominantly in the pelvis and spine (Fig. 11.6). The purely blastic lesions are less avid, and the mixed lytic and sclerotic lesions demonstrate more intense metabolic activity. Mixed lytic and sclerotic lesions are seen at the posterior aspect of the right iliac bone, sacrum, and T8 vertebral body.

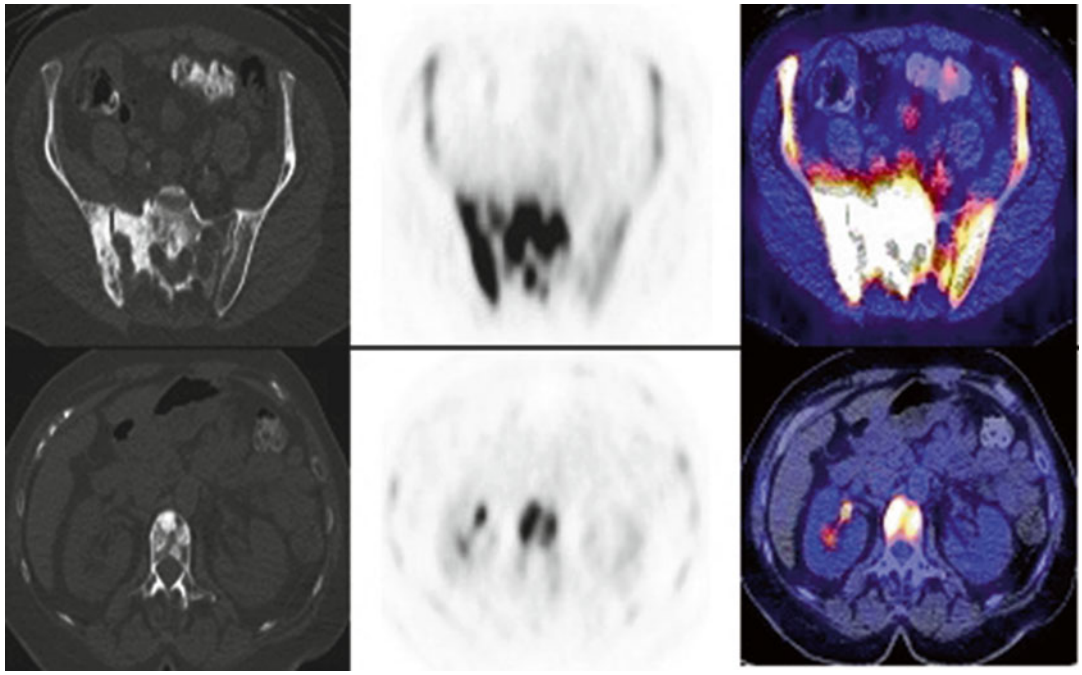

Fig. 11.6

Case 11.7 A 67-year-old female with history of metastatic breast cancer presenting with numerous osseous metastatic lesions involving the sternum, multiple ribs, L1 vertebral body, and left distal humerus (Fig. 11.7).

Lung Cancer

Case 11.8 A 25-year-old male with history of metastatic squamous cell carcinoma of the lung presenting with several hypermetabolic, predominantly lytic lesions involving multiple levels of the cervical, thoracic, and lumbar spine, manubrium and sternum, multiple ribs bilaterally, scapulae, bilateral iliac bones, sacrum, acetabulae, and ischial and pubic bones (Fig. 11.8). There is sparing of the osseous structures of the upper and lower extremities bilaterally.

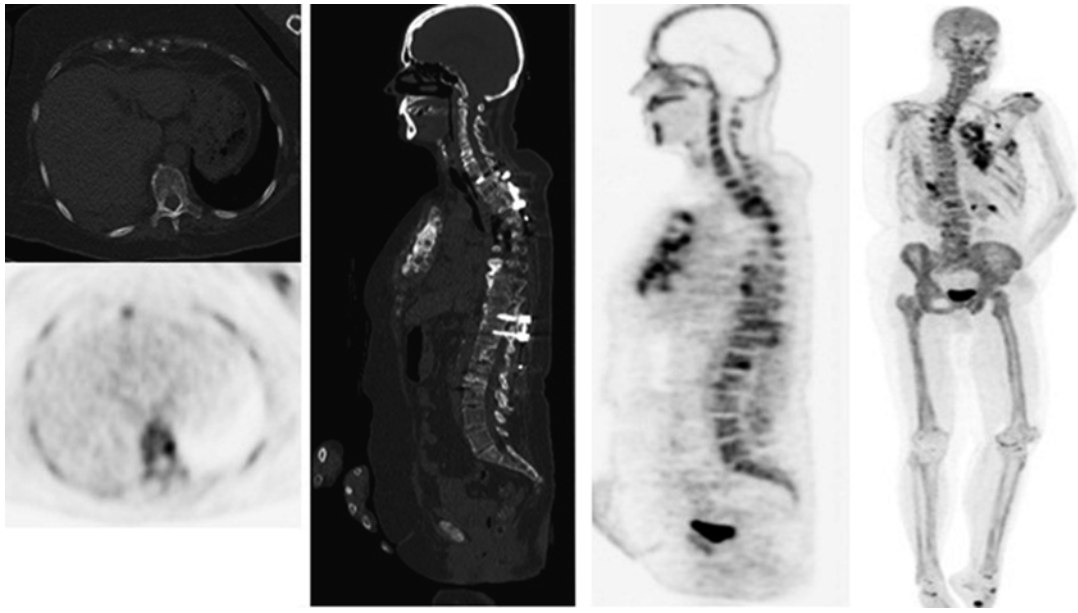

Fig. 11.7

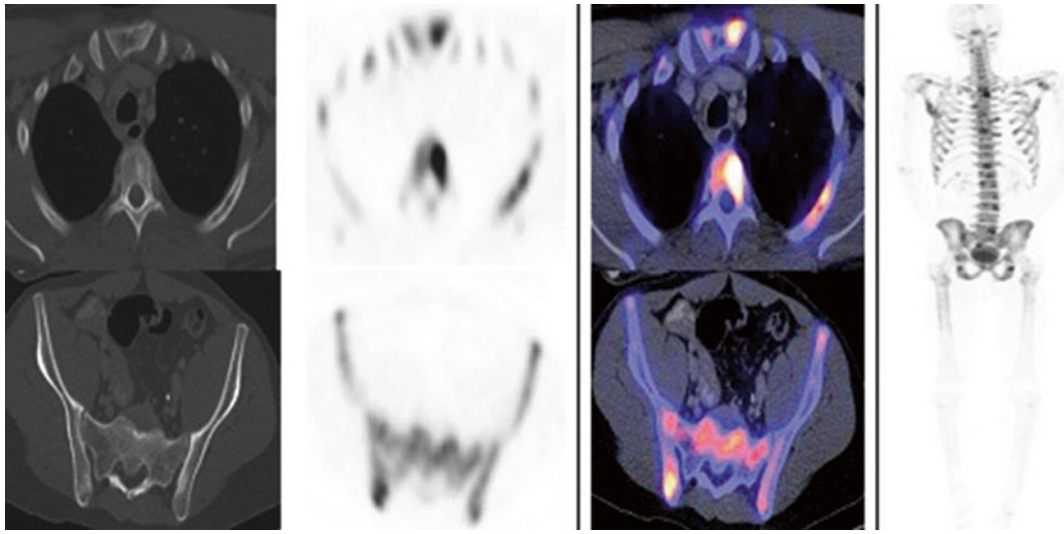

Fig. 11.8

Case 11.9

A 56-year-old male with history of metastatic adenocarcinoma of the lung, presenting with multiple sclerotic and hypermetabolic osseous lesions (Fig. 11.9). These include lesions in medial head of the left clavicle, lower sternum, and T3 vertebral body.

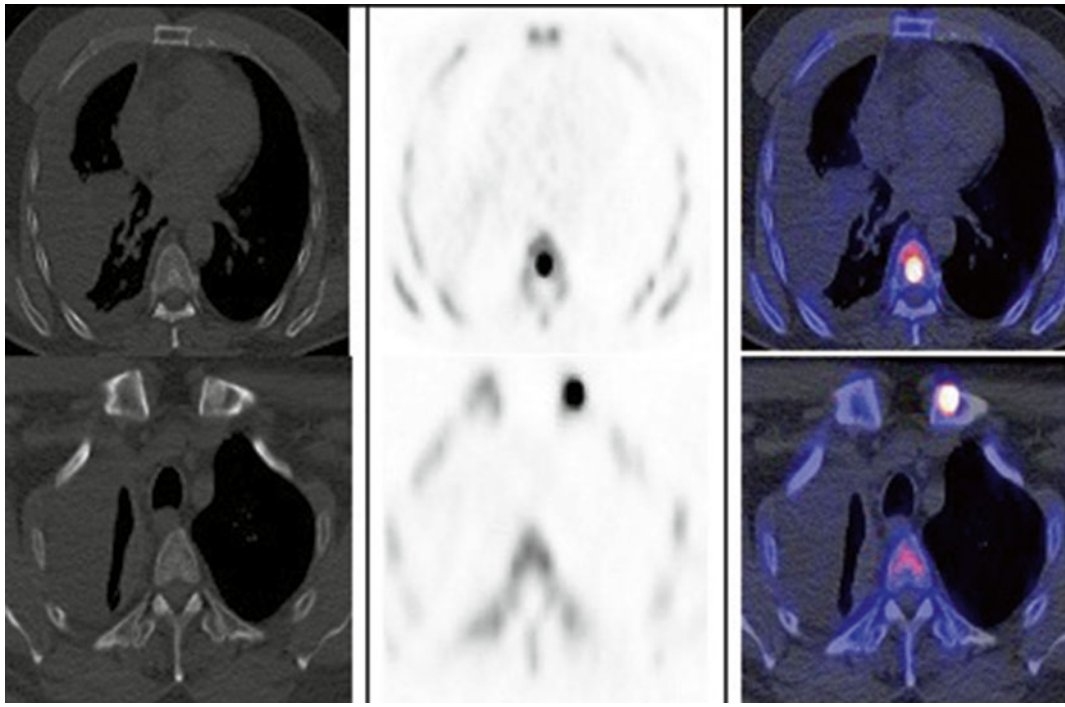

Fig. 11.9

Additional Benign Findings

Case 11.10 (1) Enthesopathic changes, (2) degenerative changes in glenohumeral joint, (3) osteophyte activity in lower thoracic spine, (4) knee arthroplasties, and (5) degenerative disc disease at L3–L4 (Fig. 11.10).

Pearls and Pitfalls

- NaF PET/CT is significantly more accurate than conventional Tc99m MDP bone scintigraphy, SPECT bone scan, and NaF PET only. Sensitivity, specificity, PPV, and NPV: planar BS (70 %, 57 %, 64 %, 55 %), SPECT BS (92 %, 82 %, 86 %, 90 %), NaF PET only (100 %, 62 %, 74 %, 100 %), and NaF PET/CT (100 %, 100 %, 100 %, 100 %) [5].
- 18F-NaF PET/CT superior to standard BS for detection of osteolytic lesions [9].
- NaF PET/CT imaging can be used for evaluation of stress relate injuries and child abuse [8].
- Very early bone reaction in small bone metastases can be seen with 18F-fluoride scintigraphy [2].
- Fluoride studies can reduce the number of invasive bone biopsies and facilitate subsequent follow-up in patients with metabolic bone disease.

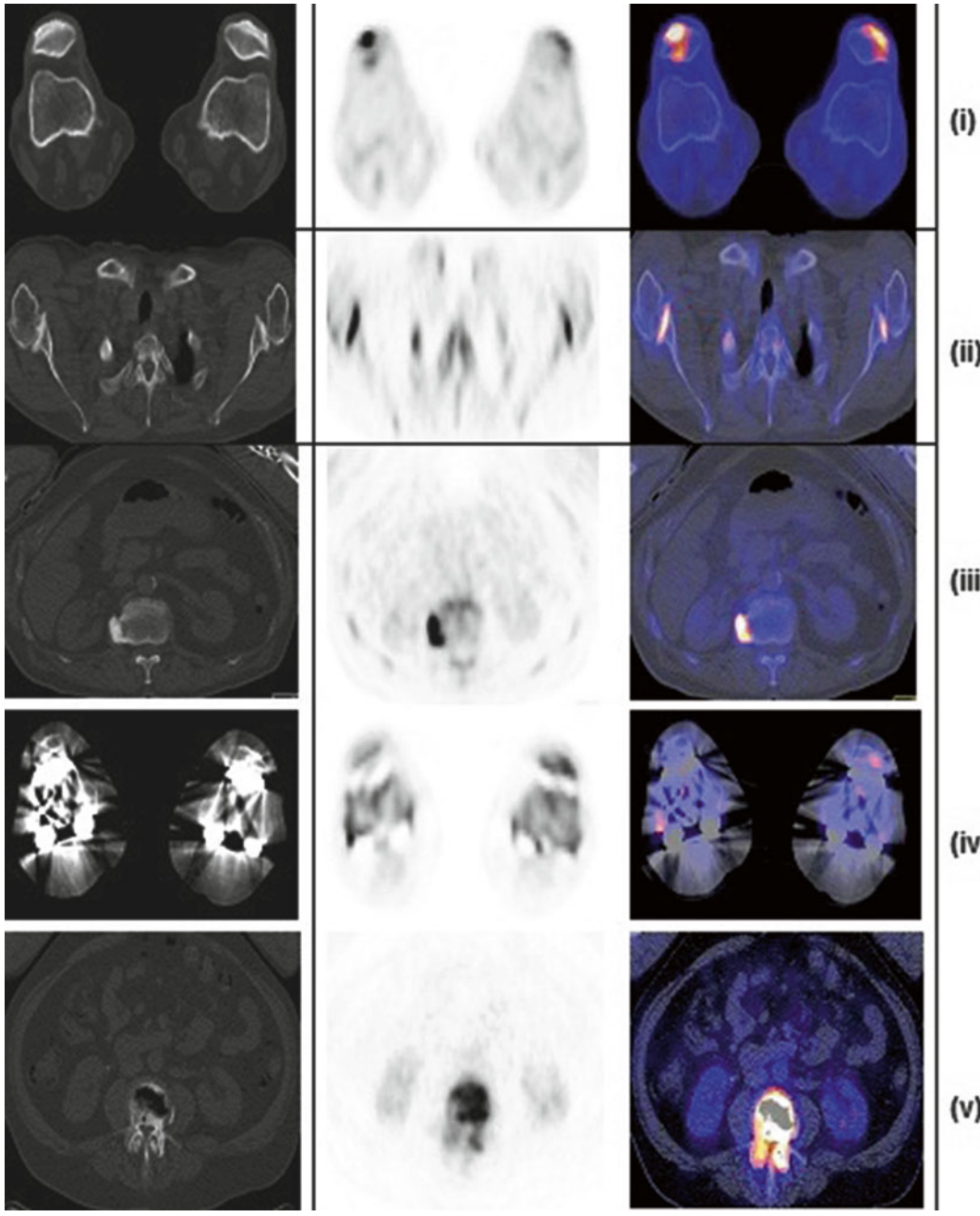

Fig. 11.10

Discussion

At least 99 % of whole-body fluoride is thought to be present in the skeleton, primarily as fluorapatite. 18F-NaF was initially introduced in 1962 as an imaging agent for bone lesions. 18F-fluoride has favorable tracer kinetics as a radiopharmaceutical for bone imaging: it accumulates in bone rapidly to a high concentration and clears quickly from the circulation, allowing a high bone-to-background uptake ratio within a short time [11]. The interest in 18F-fluoride as a bone imaging agent was renewed in the 1990s owing to a wider availability and improved technology of PET scanners, which offer higher spatial resolution and sensitivity than conventional gamma cameras used in planar scintigraphy or single-photon emission computerized tomography (SPECT). In most cases where different imaging modalities were compared, 18F-NaF PET proved to be more sensitive and specific than other techniques. Diagnostic imaging has played a major role in the evaluation of patients with bone metastases, and this application is the focus of the majority of the recent published literature on use of 18F-fluoride PET. For the detection of bone metastases in cancer patients, doses typically ranged from 8 to 12 mCi [12]. In this dose range, excellent image quality with higher spatial resolution than convention BS is obtained. There is evidence that 18F-fluoride PET is more sensitive and selective than conventional BS for diagnosis and detection of bone metastases. The use of low-dose CT in conjunction with 18F-fluoride PET improves sensitivity and specificity and improves the ability to distinguish benign from malignant lesions. Because of these advantages, and advancements in cost-effectiveness, it has been suggested that 18F-fluoride PET will replace conventional bone scan for the detection of bone metastases within several years. In summary, evidence from published studies in cancer patients indicates that 18F-fluoride PET is superior to 99mTc-MDP planar scintigraphy or SPECT in detecting primary bone cancer and skeleton metastases from a wide range of cancers, including cancer of the breast, lung, and prostate [1, 3, 4, 6, 10, 13, 14]. The very high resolution and target-to-background contrast of 18F-fluoride PET can potentially reduce its specificity; however, correlating PET with CT findings substantially helps differentiate malignant from benign lesions. 18F-fluoride PET is also effective in other applications involving altered osteogenic activity, such as detecting skeletal injury, diagnosing causes of back pain, diagnosing osteoporosis, and monitoring effectiveness of bone regeneration therapy, and in cases of child abuse [7].

References

1. Schirrmeister H, et al. Early detection and accurate description of extent of metastatic bone disease in breast cancer with fluoride ion and positron emission tomography. J Clin Oncol. 1999;17:2381–9.
2. Cook GJ, et al. The role of positron emission tomography in the management of bone metastases. Cancer. 2000;88:2927–33.

3. Blake GM, et al. Quantitative studies of bone with the use of 18F-fluoride and 99mTc-methylene diphosphonate. Semin Nucl Med. 2001;31:28–49.
4. Hetzel M, et al. F-18 NaF PET for detection of bone metastases in lung cancer: accuracy, cost-effectiveness, and impact on patient management. J Bone Miner Res. 2003;18:2206–14.
5. Even-Sapir E, et al. Assessment of malignant skeletal disease: initial experience with 18F-fluoride PET/CT and comparison between 18F-fluoride PET and 18F-fluoride PET/CT. J Nucl Med. 2004;45:272–8.
6. Even-Sapir E, et al. The detection of bone metastases in patients with high-risk prostate cancer: 99mTc MDP planar bone scintigraphy, single and multi-filed-of-view SPECT, 18F-fluoride PET and 18F-fluoride PET/CT. J Nucl Med. 2006;47:287–97.
7. Sterner T, et al. The role of [18F] fluoride positron emission tomography in the early detection of aseptic loosening of total knee arthroplasty. Int J Surg. 2007;5:99–104.
8. Beheshti M, et al. Detection of bone metastases in patients with prostate cancer by 18F fluorocholine and 18F fluoride PET-CT: a comparative study. Eur J Nucl Med Mol Imag. 2008;35:1766–74.
9. Grant F, et al. Skeletal PET with 18F-Fluoride: applying new technology to an old tracer. J Nucl Med. 2008;49:68–78.
10. Kruger S, et al. Detection of bone metastases in patients with lung cancer: ^{99m}Tc-MDP planar bone scintigraphy, ^{18}F-fluoride PET or ^{18}F-FDG PET/CT. Eur J Nucl Med Mol Imaging. 2009;36:1807–12.
11. Czernin J. Molecular mechanisms of bone 18F-NaF deposition. J Nucl Med. 2010;51:1826–9.
12. Segall G, et al. SNM practice guideline for sodium 18F-fluoride PET/CT. J Nucl Med. 2010;51:1813–20.
13. Withofs N, et al. 18F-fluoride PET/CT for assessing bone involvement in prostate and breast cancers. Nucl Med Commun. 2010;32:168–76.
14. Iagaru A, et al. Prospective evaluation of Tc99m MDP scintigraphy, 18F NaF PET/CT and 18F FDG PET/CT for detection of skeletal metastases. Mol Imaging Biol. 2011;14:252–9.